Voltammetric Study of Proton-Gated Electron Transfer in a Mutant Ferredoxin. Altering Aspartate to Asparagine Blocks Oxidation of the [3Fe–4S] Cluster of *Azotobacter vinelandii* Ferredoxin I

Julea N. Butt,† Artur Sucheta,† Lisandra L. Martin,‡,§ Binghui Shen,‡ Barbara K. Burgess,‡ and Fraser A. Armstrong*,†,∥

Department of Chemistry and Department of Molecular Biology and Biochemistry University of California, Irvine, California 92717

Received July 26, 1993

Coupling of electron transfer to a "chemical" process such as ion/molecule transfer or conformational change holds particular importance in biology for controlling reaction pathways and transducing energy.[1–4] The basis for analyzing gated (directional) electron–transfer reactions is a square (or triangular) scheme, in which electron transfer and chemical reactions combine as a thermodynamic cycle.[5–7] Electrochemical potential–reversal methods such as cyclic voltammetry thus offer an excellent way to visualize and untangle the interlinked kinetics and energetics of many of these systems.[7–9]

In redox-driven "proton pumps" [3] or enzymes such as hydrogenases or nitrogenases,[2,10] electron transfer is coupled to proton transfer. Key questions include the varied nature and characteristics of coupling and the manner by which protons are transferred through proteins. Studies using site-directed mutagenesis are important in identifying the groups that mediate proton transfer.[11] Here we present a voltammetric study of the redox kinetics of a mutant ferredoxin that appears to be kinetically defective with regard to coupled proton transfer. Configuration of the protein molecules as a nondiffusing, electroactive monolayer facilitates temporal resolution of events and enables visualization of some interesting aspects of gated reactions.

The 7Fe ferredoxin I (Fd I) from *Azotobacter vinelandii* has been extensively characterized by X-ray crystallography and spectroscopy.[12–15] The [3Fe–4S] cluster is unusual in that the one-electron-reduced form [3Fe–4S]^0 exists in either of two spectroscopically distinct states depending upon pH.[15,16] No such pH effect is observed for the oxidized [3Fe–4S]$^+$ cluster. The pH dependence of the reduction potential $E^{\circ\prime}$ suggests uptake of a single proton with pK ~ 7.8. It has been concluded that the proton binds directly at the [3Fe–4S]^0 cluster, most likely to a μ_2-sulfide.[17]

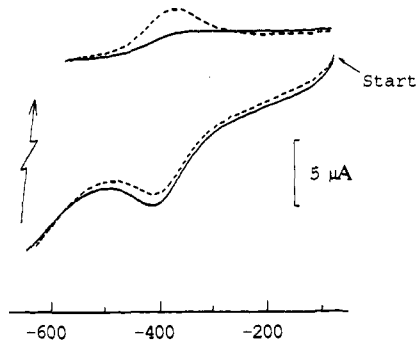

Figure 1. Initial-sweep voltammograms of films of D15N (solid line) and native (dashed line) forms of *A. vinelandii* Fd I measured at a scan rate of 930 mV s^{-1}. Capacitance background has been largely subtracted to save space, but faradaic features remain as observed, i.e., without any attempt to correct for background slope.

Scheme I describes the overall redox reaction.[18] At high pH, $E^{\circ\prime}$ ($E^{\circ\prime}_{alk}$) is independent of pH whereas at low pH, the protonation equilibrium lies far to the right and $E^{\circ\prime}$ is pH-dependent. The [3Fe–4S] cluster is buried ca. 8 Å beneath the closest solvent-accessible surface,[12] where the carboxylate group of aspartate-15 (D15) is salt-bridged to a lysine (K84).[13] We have changed D15 to asparagine by site-directed mutagenesis.[17] In the resulting D15N mutant, the salt bridge to K84 is broken, but otherwise, crystallographic and spectroscopic studies show that the structure and unusual proton-binding properties of the [3Fe–4S] cluster are conserved.[13,17] In either case, the minimum distance between the cluster (one of the μ_2-S atoms) and the carboxyl (D15) *or* carbamide (N15) O atom is 4.8 Å.[13,17] Thermodynamically, the effect of the change is moderate; the pK of the cluster is lowered to 6.9 and $E^{\circ\prime}_{alk}$ is raised from –430 mV to –409 mV.[17,19]

Scheme I

$$[3Fe\text{–}4S]^+ \underset{(k_s)}{\overset{+e^-}{\rightleftharpoons}} [3Fe\text{–}4S]^0 \underset{(k_{on},k_{off})}{\overset{+H^+}{\rightleftharpoons}} [3Fe\text{–}4S]^0\text{–}H^+$$

In terms of redox *kinetics*, however, native and D15N forms exhibit dramatically different behavior. Figure 1 shows the

† Department of Chemistry.
‡ Department of Molecular Biology and Biochemistry.
§ On leave of absence from School of Physical Sciences, Flinders University, Adelaide 5001, Australia.
∥ Present address: Inorganic Chemistry Laboratory, South Parks Road, Oxford OX1 3QR, U.K.

(1) Williams, R. J. P. *Biochim. Biophys. Acta* **1991**, *1058*, 71–74.
(2) Miller, R. W.; Smith, B. E.; Eady, R. R. *Biochem. J.* **1993**, *291*, 709–711. Wolle, D.; Dean, D. R.; Howard, J. B. *Science* **1992**, *258*, 992–994.
(3) See, for example: Chan, S. I.; Li, P. M. *Biochemistry* **1990**, *29*, 1–12. Wikström, M.; Babcock, G. T. *Nature* **1992**, *356*, 301–309.
(4) Zhou, J. S.; Kostić, N. *J. Am. Chem. Soc.* **1992**, *114*, 3562–3563 and references given.
(5) Hoffman, B. M.; Ratner, M. A. *J. Am. Chem. Soc.* **1987**, *109*, 6237–6243 (see *J. Am. Chem. Soc.* **1988**, 110, 8267 for corrections). Brunschwig, B. S.; Sutin, N. *J. Am. Chem. Soc.* **1989**, *111*, 7454–7465.
(6) Bond, A. M.; Oldham, K. B. *J. Phys. Chem.* **1983**, *87*, 2492–2502. Evans, D. H.; O'Connell, K. M. *Electroanal. Chem.* **1986**, *14*, 113–207.
(7) Laviron, E.; Rouiller, L. *J. Electroanal. Chem.* **1985**, *186*, 1–15.
(8) See: Barker, P. D.; Mauk, A. G. *J. Am. Chem. Soc.* **1992**, *114*, 3619–3624. Bixler, J.; Bakker, G.; McLendon, G. *J. Am. Chem. Soc.* **1992**, *114*, 6938–6939.
(9) Butt, J. N.; Sucheta, A.; Armstrong, F. A.; Breton, J.; Thomson, A. J.; Hatchikian, E. C. *J. Am. Chem. Soc.* **1993**, *115*, 1413–1421.
(10) Kim, J.; Rees, D. C. *Nature* **1992**, *360*, 553–560.
(11) Feher, G. *Annu. Rev. Biochem.* **1992**, *61*, 861–896 and references given.
(12) Soman, J.; Iismaa, S.; Stout, C. D. *J. Biol. Chem.* **1991**, *266*, 21558–21562.
(13) Stout, C. D. *J. Biol. Chem.*, in press.
(14) Stephens, P. J.; Jensen, G. M.; Devlin, F. J.; Morgan, T. V.; Stout, C. D.; Martin, A. E.; Burgess, B. K. *Biochemistry* **1991**, *30*, 3200–3209. Johnson, M. K.; Bennett, D. E.; Fee, J. A.; Sweeney, W. V. *Biochim. Biophys. Acta* **1987**, *911*, 81–94.
(15) Iismaa, S. E.; Vázquez, A. E.; Jensen, G. M.; Stephens, P. J.; Butt, J. N.; Armstrong, F. A.; Burgess, B. K. *J. Biol. Chem.* **1991**, *266*, 21563–21571.
(16) The ferredoxin from *A. chroococcum* exhibits very similar MCD spectroscopy and electrochemical properties. See: George, S. J.; Richards, A. J. M.; Thomson, A. J.; Yates, M. G. *Biochem. J.* **1984**, *224*, 247–251. Armstrong, F. A.; George, S. J.; Thomson, A. J.; Yates, M. G. *FEBS Lett.* **1988**, *234*, 107–110.
(17) Shen, B.; Martin, L. L.; Butt, J. N.; Armstrong, F. A.; Stout, C. D.; Jensen, G. M.; Stephens, P. J.; La Mar, G. N.; Gorst, C. M.; Burgess, B. K. *J. Biol. Chem.*, in press.
(18) Scheme I corresponds to two sides of a square scheme as described in refs 6 and 7. By scanning rapidly from the lower switching potential up to +200 mV, we determined that the cyclic pathway (oxidation of [3Fe–4S]^0–H$^+$, then deprotonation) is not followed.
(19) The limiting value of $E^{\circ\prime}$ at high pH is more positive, by ca. 21 mV, for the D15N mutant, consistent with stabilization of [3Fe–4S]^0 by removal of the nearby aspartate, while the pK of [3Fe–4S]^0 is decreased by ca. 0.8 pH units. The two observations are essentially equivalent. At low pH, $E^{\circ\prime}$ values for native and D15N Fd I are very similar, as expected if electron transfer is coulombically balanced by proton transfer.

0002-7863/93/1515-12587$04.00/0

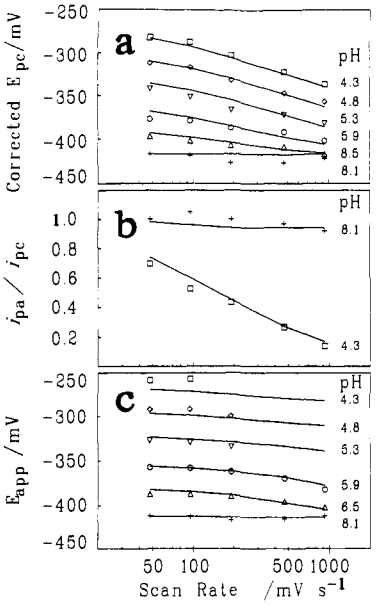

Figure 2. Scan-rate dependence of experimental (symbols) and simulated (solid lines) cathodic peak potential, E_{pc} (a), ratio of anodic-to-cathodic peak currents, i_{pa}/i_{pc} (b), and the apparent reduction potential $E^{\circ\prime}_{app}$ (c), as observed for reduction of the [3Fe–4S]$^+$ cluster of D15N ferre doxin configured as an electroactive film in contact with electrolyte at different pH values. Simulation parameters (rate constants) are given in the text.

voltammetry of native and D15N Fd I, immobilized as near-monolayer films at a pyrolytic graphite "edge" (PGE) electrode,[9,20,21] measured under conditions of pH that yield similar driving forces for protonation of [3Fe–4S]^0 (respectively pH 6.5 and 5.9).[19] As the scan rate (ν) is raised to the value 930 mV s^{-1} as shown, the faradaic response for native Fd I remains essentially reversible with little sign of complications from rate-determining coupled reactions. By contrast, the oxidation wave for D15N collapses (while the reduction peak remains large). As shown in Figure 2a, the reduction peak and (eventually to a lesser degree) the attenuated oxidation peak/wave shift to more negative potential as the scan rate is increased.

Results obtained for D15N over a wide range of pH and ν values were analyzed according to the reversible model shown in Scheme I in which electron transfer is intrinsically facile (large k_s),[22] but rates of dependent chemical processes, in this case protonation ($=k_{on}[H^+]$) and deprotonation (k_{off}) of [3Fe–4S]^0, are retarded and comparable with ν.[18,23] We used a modification of the computational procedure described recently for the case of redox-coupled ligand binding to a [4Fe–4S] cluster.[9] Rate constants k_{on} and k_{off}, as well as the standard first-order electrochemical rate constant k_s,[22] were each assumed to be independent of pH and defined as adjustable parameters in simulation-based model fitting.[23] We exploited the following observations: (a) that the position of the reduction peak E_{pc} is sharply defined and depends on pH and ν and (b) that the peak current ratio i_{pa}/i_{pc} is a function of pH, ν, and cathodic switching potential. Results are shown in Figure 2a,b. In support of the model, an excellent fit (solid lines) was obtained with $k_{on} = 3 \pm 1 \times 10^7$ M^{-1} s^{-1}, $k_{off} = 3 \pm 1$ s^{-1}, and $k_s = 500 \pm 200$ s^{-1}.

The voltammetric experiment thus allows unambiguous identification of an otherwise rapid electron-transfer reaction that is gated, in this case by a proton-dependent chemical process. The rate constants k_{on} and k_{off} for D15N are much smaller than for native Fd I, which shows little evidence for kinetic decoupling under comparable conditions.[24] From the kinetic results, and with the weight of evidence from crystallography, spectroscopy, and redox thermodynamics, we have proposed that the K84–D15 salt bridge, $NH_2H^+\cdots{}^-OOC$, facilitates proton transfer between the cluster and solvent water molecules.[17,24,25] An interesting possibility is that the bridging H$^+$ is directly involved in a proton conduction pathway.

A more subtle effect pertaining to the energetics of electron-transport systems is also demonstrated. The negative shift of E_{pc} with increasing scan rate, combined with the almost stationary value or slight negative shift of E_{pa}, produces a decrease in the reduction potential ($E^{\circ\prime}_{app} = (E_{pc} + E_{pa})/2$) as the scan rate is increased (Figure 2c).[26] In the extreme situation, if the electron is retrieved (or relayed further on) *before* the cluster can be protonated, then the "time-dependent" reduction potential ultimately reverts to the limiting value measured under alkaline conditions.[27] By their very nature, the energetics of biological electron-transport systems may stray far from conditions of equilibrium. The result underscores the expectation that transient processes in rapid electron-transport systems may be associated with reduction potentials that deviate considerably from the static values determined by potentiometry.

Acknowledgment. This work was supported by National Science Foundation Grant MCB-9118772 (to F.A.A.), a grant from the donors of the Petroleum Research Fund, administered by the American Chemical Society (to F.A.A.) and National Institutes of Health Grant GM-45209 (to B.K.B.). L.L.M. was supported in part by a Fulbright Fellowship.

Supplementary Material Available: Plots of $E^{\circ\prime}$ as a function of pH and dimensionless current as a function of potential (2 pages). This material is contained in many libraries on microfiche, immediately follows this article in the microfilm version of the journal, and can be ordered from the ACS; see any current masthead page for ordering information.

(20) Armstrong, F. A.; Butt, J. N.; Sucheta, A. *Methods Enzymol.* **1993**, *277*, 479–500.

(21) Experiments were performed at 0 °C as described in ref 20. Polymyxin or neomycin gave similar results as coadsorbates at PGE electrodes. The electrolyte consisted of 0.1 M NaCl containing acetate, MES, HEPES, TAPS (5 mM each), and 0.1 mM EGTA. All potentials were corrected to correspond to the standard hydrogen electrode (SHE). Control experiments carried out using 200 mM MES at pH 5.9 yielded results identical to those yielded by the same experiments carried out with dilute buffer.

(22) The term k_s is the standard electrochemical rate constant (units of s^{-1}) for a redox couple that is confined to the electrode surface. See, for example: Laviron, E. *J. Electroanal. Chem.* **1979**, *101*, 19–28.

(23) The model (see ref 9) assumed that electron- and proton-transfer reactions were confined to a homogeneous layer of protein molecules immobilized on the electrode surface and that the electrochemical reaction conformed to Butler–Volmer kinetics (see ref 22).

(24) Interestingly, as the pH is decreased below 6, decoupling becomes increasingly apparent for native Fd I. The onset of this behavior coincides with protonation of D15 and loss of the salt bridge to K84 (see ref 17). See also: Cheng, H.; Grohmann, K.; Sweeney, W. *J. Biol. Chem.* **1990**, *265*, 12388–12392.

(25) The close structural and spectroscopic properties of the [3Fe–4S] cluster in native and D15N forms of Fd I argue strongly against the possibility that the contrasting rate constants for proton transfer reflect different rates of electronic and nuclear reorganization at the cluster itself. See: Carroll, J. M.; Norton, J. R. *J. Am. Chem. Soc.* **1992**, *114*, 8744–8745.

(26) The scan-rate sensitivity of $E^{\circ\prime}_{app}$ within the range of this study is optimized at pH values just below the cluster pK. This effect arises since further lowering of the pH necessitates higher scan rates to compete with the increased rate of protonation ($k_{on}[H^+]$).

(27) Equivalently, and provided electron transfer remains reversible, the voltammogram should revert back to the ideal form (but displaced along the potential axis) at sufficiently high ν.